JOURNAL OF SOLID STATE CHEMISTRY **125,** 249–254 (1996)
ARTICLE NO. 0293

Two New Examples for the Unusual $R_{12}I_{17}Z_2$-Structure Type: $La_{12}I_{17}Fe_2$ and $Ce_{12}I_{17}Mn_2$

Michael Lulei, James D. Martin, and John D. Corbett

Department of Chemistry, Iowa State University, Ames, Iowa 50011

Received April 8, 1996; accepted May 30, 1996

Reactions of KI, La, LaI_3, and Fe in niobium tubes at 900°C yield black crystals of $La_{12}I_{17}Fe_2$ which were characterized by single-crystal X-ray diffraction (triclinic, $P\bar{1}$, $Z = 1$, $a = 11.967(8)$, $b = 11.851(6)$, $c = 9.918(7)$ Å, $\alpha = 114.59(5)°$, $\beta = 104.83(6)°$, $\gamma = 93.05(5)°$, $R(F)/R_w = 3.8/4.3\%$). Similar experiments also gave the isostructural $Ce_{12}I_{17}Mn_2$ according to the Guinier powder pattern ($a = 11.863(6)$, $b = 11.840(6)$, $c = 9.857(5)$ Å, $\alpha = 14.90(4)°$, $\beta = 104.47(4)°$, $\gamma = 93.28(4)°$). The $Pr_{12}I_{17}Fe_2$-type structure contains octahedral rare-earth-metal cluster units R_6 centered by a transition-metal atom Z and sheathed by iodine atoms. These are closely linked by seven I^{i-i} and one I^{i-a-a} bridges that lead to the unusually low I:Pr ratio for phases with isolated clusters. The compounds reported here together with $Pr_{12}I_{17}Z_2$, Z = Fe, Re are the only phases known to adopt this structure type. The $La_{12}I_{17}Fe_2$ phase formally has 17.5 *e* per cluster, and its magnetic susceptibility data are consistent with equal numbers of 17-*e* and 18-*e* (closed shell) clusters, with $\mu = 1.11$ BM for the former. © 1996 Academic Press, Inc.

I. INTRODUCTION

The important structural building-block in "reduced" rare-earth-metal halides is the octahedral cluster R_6 that is centered by a mandatory interstitial atom Z and bridged over each edge by halide atoms X to yield the well-known $R_6X_{12}Z$ unit (1–3). Ternary compounds with discrete cluster units that are centered by interstitial transition metal atoms are noteworthy in their low X:R ratios, reflecting the relatively low electron counts of the host R metals. Only three different structure types are known. The $R_6X_{10}Z$ (4–6) and $R_7X_{12}Z$ types (4, 7–9) form with a remarkably large variety of rare-earth-metals, interstitial elements, and halides (Cl, Br, I). On the contrary, only two examples are known for the recently discovered and particularly iodine-poor $R_{12}X_{17}Z_2$ structure type, namely $Pr_{12}I_{17}Fe_2$ and $Pr_{12}I_{17}Re_2$ (10). These compounds are unusual for both the fractional number of electrons available for the single type of cluster, 17.5 and 16.5, respectively, relative to 18 for closed shell bonding, and the close approach of separate clusters owing to the large fraction of shared inner–inner iodine bridges (I^i–I^i). The research reported here has been focused on experiments with lanthanum and cerium and a variety of interstitial elements designed to expand the variety of compounds in this system and to examine conduction prospects. Lanthanum is especially attractive as it provides a diamagnetic background.

II. EXPERIMENTAL SECTION

1. Synthesis

The synthetic and sublimation techniques for LaI_3 and CeI_3 and the reaction procedures utilizing welded Nb tubing have been described before (7, 11). La and Ce metal (Ames Laboratory), Mn (Johnson-Matthey, 99.99%), and Fe powder (Alfa, 99.5%) were used as received and handled in a glovebox. The first reaction giving this phase had the overall stoichiometry La_5I_7Fe and was heated at 900°C for 21 days, and then the furnace was turned off. The products were 85% black crystalline $La_{12}I_{17}Fe_2$, 10% LaI_2 ($MoSi_2$-type) (12), and 5% LaOI. The phase was later obtained in ≥80% yields from reactions loaded as $La_{12}I_{17}Fe_2$ (plus 10% LaI_2, 5% LaOI), $La_{14}I_{17}Fe_2$ (5% LaOI, 5% La), and $La_{12}I_{17}Fe_{1.9}$ (15% LaI_2, 5% LaOI). The phase was also observed in 40% yield in reactions with the starting stoichiometry La_2IFe_2 (besides 30% La_2IFe_2, 15% Fe, 10% La, and 5% LaOI). Parallel 900°C reactions loaded as La_5I_7Z with Z = Ru, Os, Mn, Re as well as mixed interstitials Mn/Fe, Mn/Ru, Mn/Os, Re/Os, and Re/Ru did not yield any $La_{12}I_{17}Z_2$ compounds but mainly LaI_2 and unidentified phases. Black crystals of $Ce_{12}I_{17}Mn_2$ were obtained after reactions at 750°C for 63 days with the overall stoichiometry $Ce_{18}I_9Mn_2$. The products were, besides unreacted Ce metal, 70% $Ce_{12}I_{17}Mn_2$, 20% CeI_2, and 10% CeOI. Reactions with the correct starting composition and Fe, Co, or Os as the interstitial produced only 70% of the corresponding $Ce_7I_{12}Z$ phases besides ~20% CeI_2 and ~10% CeOI. All products were characterized by Guinier powder diffraction, from which the yields of the respective compounds were so estimated.

0022-4596/96 $18.00

2. X-Ray Studies

Crystals of $La_{12}I_{17}Fe_2$ were mounted in thin-walled glass capillaries in the glovebox, and their quality was checked by Laue and oscillation photographs on Weissenberg cameras. The original cell parameters (a = 9.922(3), b = 11.827(2), c = 11.940(2), α = 74.14(1), β = 75.00(2), γ = 66.21(2)) and the orientation matrix were obtained from a least-square refinement of the setting angles of 25 centered reflections collected on a CAD4 diffractometer using graphite-monochomated Mo$K\alpha$ radiation. A total of 4519 reflections were collected ($4° \le 2\theta \le 50°$; $+h$, $\pm k$, ± 1; 2θ-ω scans) at room temperature to give 2160 unique data ($I > 3\sigma_I$, R_{avg} = 0.06) for the space group $P\bar{1}$ (no. 2) after averaging the redundant data. The lattice parameters and the data set were transformed by a matrix operation to the correct triclinic setting with all angles >90°, comparable to those of $Pr_{12}I_{17}Fe_2$ described earlier, and the latter's atom positions were then used as starting parameters for a least-square refinement for the structure. Programs, scattering factors, etc. utilized were those in the instrument package TEXSAN (13). An empirical absorption correction was applied to the full data set with the aid of four Ψ-scans and later, after isotropic refinement, with DIFABS (14) (min./max. relative transmission factors: 0.826/1.110, μ = 216.0 cm^{-1}). The residuals after the anisotropic refinement of all atoms (143 variables) were $R(F)$ = 0.038, R_w = 0.043. The largest residual peak, 2.72 Å from I1, was 2.57 e/Å^3. The Guinier powder pattern calculated for the refined structural model agreed very well with the one observed for the bulk product (with Si as internal standard) and was also used to index the powder pattern for $Ce_{12}I_{17}Fe_2$ in order to determine its lattice constants. Some data collection and refinement parameters are given in Table 1. The final atomic coordinates, isotropic-equivalent and anisotropic temperature factors, and their estimated standard deviations are listed in Tables 2 and 3. The structure factor data are available from J.D.C.

3. Magnetic Measurements

A sample of $La_{12}I_{17}Fe_2$ (35 mg) was sealed within an improved fused silica susceptibility container (15) under He in a glove box. The sample magnetization was first checked as a function of the applied field between 0.1 and 5.5 T at 25, 50, 100, 150, 200, 250, and 300 K to assess

TABLE 1
Crystallographic Data for $La_{12}I_{17}Fe_2$

Crystal data	
Formula	$La_{12}I_{17}Fe_2$
Crystal color, habit	Black, irregular
Crystal system, space group, Z	Triclinic, $P\bar{1}$, 1
Lattice constants (Å)[a]	a = 11.967(8), b = 11.851(6), c = 9.918(7) α = 114.59°, β = 104.83(6)°, γ = 93.05(5)°
V (Å^3)	1215(3)
D_{calc} (g/cm^3)	5.38
μ (Mo$K\alpha$, cm^{-1})	216.0
Data collection	
Diffractometer	Enraf-Nonius CAD4
Radiation, λ (Å)	Mo$K\alpha$, 0.70958
Scan type	ω-2θ
Temperature	23°C
Octants measured, $2\theta_{max}$	$+h$, $\pm k$, ± 1 to 50°
Refinement	
Measured reflections	4519
Independent reflections	4252
Unique reflections $I > 3\sigma_I$	2610
Number of variables	143
Absorption corrections	Empirical, 4 Ψ-scans; DIFABS
Transm. coeff. range	0.826–1.110
Sec. ext. coeff.	3.6(4) $\times$ 10^{-8}
$R_{avg}(I > 0)$	0.06
Largest residual peak (e/Å^3)	2.57 (2.72 Å from I1)
R, R_w[b]	0.038, 0.043

[a] From 34 reflections measured in Guinier powder pattern at 22°C, λ = 1.54056 Å.
[b] $R = \Sigma||F_0| - |F_c||/\Sigma|F_0|$, $R_w = [\Sigma w(|F_0| - |F_c|)^2/\Sigma wF_0^2]^{1/2}$, $w = \sigma_F^{-2}$.

TABLE 2
Positional and Isotropic Equivalent Displacement Parameters (Å²) for $La_{12}I_{17}Fe_2$

Atom	x	y	z	B_{eq}[a]
La1	0.1509(1)	0.2881(2)	0.1494(2)	1.77(5)
La2	0.3294(1)	0.5205(1)	0.0689(2)	1.46(5)
La3	0.2794(1)	0.2387(2)	0.6421(2)	1.72(5)
La4	0.4215(1)	0.1843(2)	0.0087(2)	1.48(5)
La5	0.0007(1)	0.3354(2)	0.7756(2)	1.83(5)
La6	0.0946(1)	0.0038(2)	0.7216(2)	2.04(6)
I1	0.0	0.0	0.0	4.1(1)
I2	0.4108(2)	0.5306(2)	0.7766(2)	1.66(7)
I3	0.1740(2)	0.9405(2)	0.4049(2)	2.29(8)
I4	0.3175(2)	0.8865(3)	0.8354(3)	2.9(1)
I5	0.2547(2)	0.5874(2)	0.3802(2)	2.07(8)
I6	0.1120(2)	0.6420(3)	0.9408(3)	1.89(8)
I7	0.4630(2)	0.8328(3)	0.2597(3)	2.05(8)
I8	0.3749(2)	0.2102(4)	0.3295(3)	2.90(8)
I9	0.0457(2)	0.3093(3)	0.4535(3)	2.10(7)
Fe	0.2129(5)	0.2617(7)	0.8952(7)	1.36(9)

[a] $B_{eq} = (8\pi^2/3)\Sigma_i\Sigma_j U_{ij} a_i^* a_j^* \vec{a}_i \vec{a}_j$.

possible ferromagnetic and paramagnetic impurities, and then the sample was measured at 0.5, 1, and 3 T over a range 2–300 K on a Quantum Design SQUID magnetometer. Data were corrected for the susceptibility of the container and for the estimated core diamagnetism, -1.15×10^{-3} emu mol^{-1}.

III. RESULTS AND DISCUSSION

The two new compounds $La_{12}I_{17}Fe_2$ and $Ce_{12}I_{17}Mn_2$ crystallize triclinic in the space group $P\bar{1}$. Their lattice parameters together with those of the isotypic structures $Pr_{12}I_{17}Fe_2$ and $Pr_{12}I_{17}Re_2$ are listed in Table 4. The cell volumes show the expected differences. The La phase has the largest cell volume, followed by the Ce and the Pr representatives, with a slight decrease in the last between the Re and the Fe interstitials.

An important structure feature of all compounds is the octahedral rare-earth-metal cluster R_6 formed by six crystallographically distinct metal atoms and centered by a transition metal atom such as Fe, Mn, or Re. Important interatomic distances are listed in Table 5. In the structure of $La_{12}I_{17}Fe_2$, the La1–Fe (2.71 Å) and La3–Fe (2.74 Å) separations are distinctively shorter ($\Delta\overline{d} = 0.13$ Å) than the La2–Fe, La4–Fe, La5–Fe, and La6–Fe distances (2.87, 2.83, 2.86, and 2.87 Å, respectively; $\sigma < 0.01$ Å). This presents a significant contrast to the Pr–Fe separations in $Pr_{12}I_{17}Fe_2$ in which $\Delta\overline{d}$ is only 0.03 Å for the same groups. Therefore, the octahedron in $La_{12}I_{17}Fe_2$ is much more compressed along the La1–Fe–La3 axis. The average of the 12 independent La–La distances is 3.98 Å with a range from 3.86 Å for La1–La2 to 4.08 Å for La2–La5. It is difficult to find reasons for the distortions of the La_6Fe unit in terms of either electronic factors or matrix effects by the halide atoms. The shortest d(I–I) is 4.17 Å, which is not at all unusual, so angular effects at intercluster bridging in this complex low-symmetry array must be responsible. Interestingly, the shortest intercluster distance La6–La6 is surprisingly small, 4.36 Å, and is one indication of how closely the clusters are packed within the structure.

Improved aids to the overall visualization of this complex structure are provided as Figures 1 and 2. The first shows a perspective view along [010] of the spatial arrangement of the La_6Fe clusters in and around the unit cell with the

TABLE 3
Anisotropic Temperature Factors (Å²)[a] for $La_{12}I_{17}Fe_2$

Atom	U_{11}[a]	U_{22}	U_{33}	U_{12}	U_{13}	U_{23}
La1	0.0193(8)	0.023(1)	0.026(1)	0.0050(7)	0.0063(7)	0.0125(8)
La2	0.0201(8)	0.0180(9)	0.0192(8)	0.0041(7)	0.0072(6)	0.0092(7)
La3	0.0219(8)	0.153(8)	0.024(1)	−0.0012(6)	0.0026(7)	0.0087(8)
La4	0.0187(9)	0.020(1)	0.0191(8)	0.0042(7)	0.0062(7)	0.0100(7)
La5	0.0221(8)	0.025(1)	0.0212(8)	0.0008(7)	0.0048(6)	0.0103(7)
La6	0.028(1)	0.026(1)	0.034(1)	0.0098(8)	0.0173(7)	0.0181(8)
I1	0.083(3)	0.035(2)	0.034(2)	−0.017(2)	0.033(2)	0.008(2)
I2	0.019(1)	0.019(1)	0.022(1)	−0.0010(9)	0.0032(8)	0.008(1)
I3	0.033(1)	0.019(1)	0.027(1)	0.001(1)	0.010(1)	0.003(1)
I4	0.032(2)	0.018(2)	0.051(2)	0.007(1)	0.003(1)	0.012(1)
I5	0.028(1)	0.029(2)	0.019(1)	0.004(1)	0.006(1)	0.008(1)
I6	0.018(1)	0.028(2)	0.026(1)	0.007(1)	0.005(1)	0.014(1)
I7	0.025(1)	0.027(1)	0.028(1)	0.007(1)	0.013(1)	0.010(1)
I8	0.033(1)	0.064(2)	0.032(1)	0.023(1)	0.017(1)	0.034(1)
I9	0.025(1)	0.033(1)	0.020(1)	0.004(1)	0.0060(9)	0.012(1)
Fe	0.016(1)	0.019(2)	0.018(1)	0.005(1)	0.005(1)	0.009(1)

[a] $U_{ij} = \exp\{-2\pi^2(U_{11}h^2a^{*2} + \cdots + U_{23}klb^*c^*)\}$.

TABLE 4
Lattice Constants (in Å) of Compounds with the $R_{12}I_{17}Z_2$ Structure Type[a]

Compound	a	b	c	α	β	γ	v (Å^3)
$Pr_{12}I_{17}Fe_2$	11.798(4)	11.791(2)	9.830(2)	114.87(2)°	104.82(4)°	93.19(2)°	1178(1)
$Pr_{12}I_{17}Re_2$	11.870(3)	11.770(9)	9.835(4)	114.29(3)°	104.90(2)°	93.20(3)°	1190(2)
$Ce_{12}I_{17}Mn_2$	11.863(6)	11.840(6)	9.857(5)	114.90(4)°	104.47(4)°	93.28(4)°	1195(2)
$La_{12}I_{17}Fe_2$	11.967(8)	11.851(6)	9.918(7)	114.59(5)°	104.83(6)°	93.05(5)°	1215(3)

[a] From the respective Guinier powder patterns with Si as internal standard, $\lambda = 1.54056$ Å, and a minimum of 32 reflections each.

La atoms numbered, while Fig. 2 shows an infinite [010] view of all atoms around the a–c face, illustrating all bridging iodine atoms and their functions in this complicated three-dimensional structure. All clusters are equivalent and related either by translation or inversion. All 12 edges of the rare-earth-metal octahedron are bridged by one of nine crystallographically different iodine atoms to form the well known R_6X_{12} unit common to most rare-earth-metal clusters. Inversion centers at 0,0,0 (I1), on the b–c face, and on the c edge generate all of the inner–inner (I^{i-i}) bridging functions of I1, I2, I3, and I6. Pairs of I^{i-a}–I^{a-i} intercluster bridges by I4, I5, I8 as well as the unusual I9 as I^{i-a-a} also surround either the foregoing I^{i-i} atoms or $\frac{1}{2},\frac{1}{2},\frac{1}{2}$, as follows.

I1 atoms at the origins cover the La1–La6 edges and link two clusters together as I^{i-i}. Each cluster has two 12 atoms with the functionality I^{i-i} related by an inversion center on the a–c face. The pair bridge La2–La3 and La2–La4 edges on one cluster and bond to the opposite members on the adjacent cluster. The connectivities of I3 and I6 are similar I2. Pairs of I3 atoms related by inversion at 0, 0, $\frac{1}{2}$ (the c edge) connect La3–La6 and La5–La6 edges while I6 pairs about the origin tie La1–La5 and La2–La5 edges of neighboring octahedra together. Figure 2 also shows how I4, I5, I7, and I8 as I^{i-a} bridge each La4–La6, La–1–La2, La3–La4, and La1–La4 edge of the metal octahedra and in addition form exo bonds, to La4, La5, La2, and La3, respectively, to interconnect the clusters. Each is generally opposed by an inversion-related equivalent iodide I^{a-i} that links the same cluster pairs. These are matched (see Fig. 2) with parallel I^{i-i} functions, I4 and I7 and I2, I5 with I2, I5 with I1 and I6, while I8 pairs are best related just by the body-center inversion center. Finally, I9 atoms with their unique I^{i-a-a} functionality bridge the remaining La3–La5 edge and in addition form exo bonds to a La6 and a La1 atom in two different clusters. These connect three clusters at the same time in parallel with the $I3^{i-i}$ functions. Therefore, the oveall interconnection pattern of the iodine atoms can be formulated as $[La_6(Fe)]I_7^{i-i}I^{i-a}{}_{4/2}I^{a-i}{}_{4/2}I^{i-a-a}$. The La–I distances are typical for the functions of the iodine atoms. Separations with I^i character have average La–I distances of 3.28 Å, while those with exo bonds of I^a type average 3.45 Å.

Electron counting for cluster bonding in $La_{12}I_{17}Fe_2$ ($12 \cdot 3 - 17 \cdot 1 + 2 \cdot 8$) shows that there are 35 e^- available for metal–metal bonding, or 17.5 e^- per average La_6Fe cluster. Presumably 17- and 18-electron clusters are in fact actually present in some disordered manner, the latter being closed-shell. The thermal ellipsoids of the rare-earth-metals, particularly in $Pr_{12}I_{17}Fe_2$, are quite normal in size relative to those of other cluster iodides (16, 17), suggesting that a distinguishable superstructure is not present at room temperature. Proof of the presence of one unpaired elec-

TABLE 5
Important Interatomic Distances (Å) for $La_{12}I_{17}Fe_2$

Fe–La1	2.709(6)	I3–La3	3.272(4)
Fe–La2	2.869(8)	I3–La5	3.279(4)
Fe–La3	2.735(6)	I3–La6	3.313(4)
Fe–La4	2.829(7)	I3–La6	3.346(4)
Fe–La5	2.859(7)		
Fe–La6	2.868(8)	I4–La4	3.218(4)
		I4–La4	3.426(4)
La1–La2	3.855(3)	I4–La6	3.237(4)
La1–La4	3.906(3)		
La1–La5	3.964(4)	I5–La1	3.269(4)
La1–La6	4.026(5)	I5–La2	3.226(3)
La2–La3	4.019(4)	I5–La5	3.410(4)
La2–La4	4.003(3)		
La2–La5	4.082(5)	I6–La1	3.292(4)
La3–La4	3.927(4)	I6–La2	3.269(4)
La3–La5	3.949(3)	I6–La5	3.328(4)
La3–La6	3.915(3)	I6–La5	3.340(3)
La4–La6	4.041(5)		
La5–La6	4.003(3)	I7–La2	3.439(4)
La6–La6[a]	4.361(5)	I7–La3	3.255(4)
		I7–La4	3.241(4)
I1–La1	2 × 3.298(3)		
I1–La6	2 × 3.256(3)	I8–La1	3.227(4)
		I8–La3	3.466(4)
I2–La2	3.303(3)	I8–La4	3.263(4)
I2–La2	3.331(3)		
I2–La3	3.275(4)	I9–La1	3.476(4)
I2–La4	3.329(4)	I9–La3	3.301(4)
		I9–La5	3.267(4)
		I9–La6	3.476(5)

[a] Shortest intercluster distance.

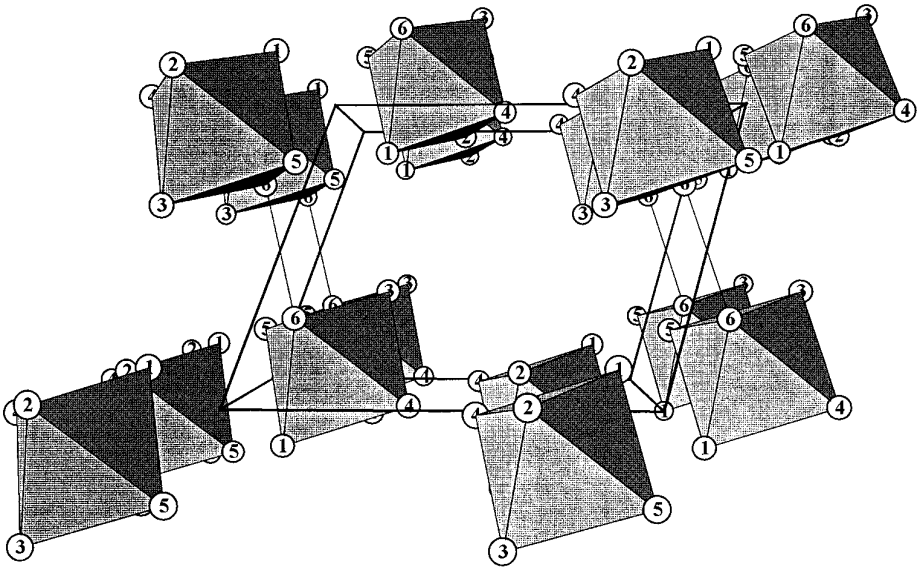

FIG. 1. $La_{12}I_{17}Fe_2$: A perspective view along [010] of the isolated La_6Fe octahedra in the triclinic unit cell to show the spatial arrangement. The original lies in the lower right corner with c approximately vertical. (La atoms are numbered; lines between La6 atoms mark the shortest intercluster separations (4.36 Å.)

tron per formula unit was found in the magnetic susceptibility data. The $M(T)$–H (magnetization–field) data indicated the presence of a ferromagnetic impurity, possibly iron, as well as paramagnetic impurities that affected M vs H only at lower fields and below ~100 K. An appreciable temperature-independent (van Vleck) contribution also seemed evident in the data, especially at the higher temperatures. In view of these complexities, the magnetization data at 3 T were corrected for the ferromagnetic content (1.2×10^{-4} emu, equivalent to 0.6 μg or 2×10^{-3} wt% Fe), and χ then was fit over 100–300 K by the nonlinear function $\chi = C/(T - \theta) + \chi_0$ with $C = 0.154(3)$ emu mol^{-1}, $\theta = -4(1)$ K, and $\chi_0 = 1.519(3) \times 10^{-3}$ emu mol^{-1}. The temperature dependence of the corrected molar suscepti-

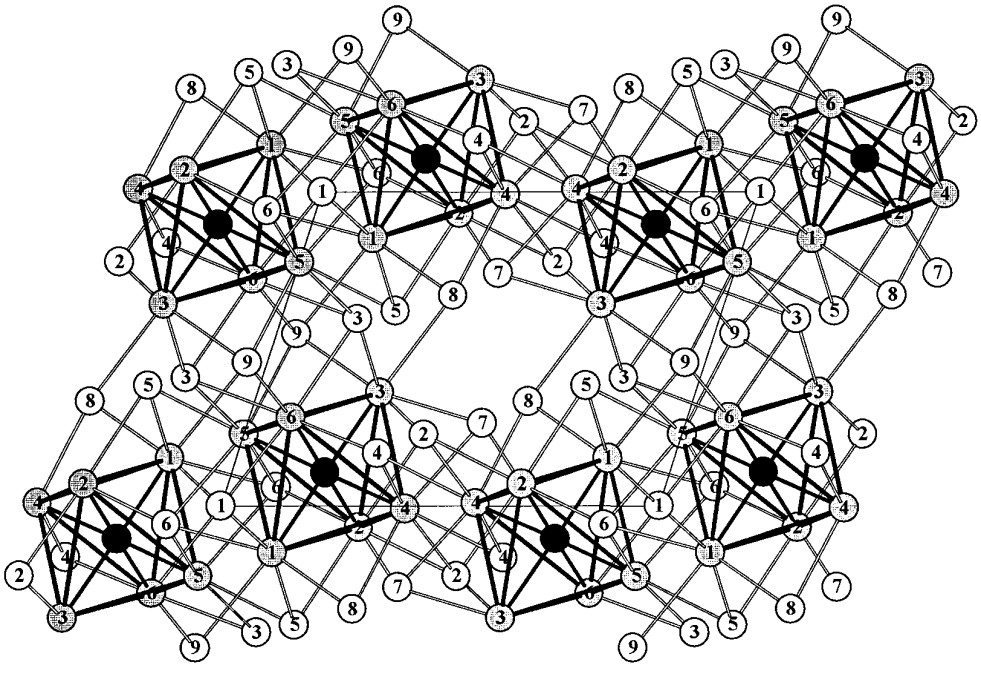

FIG. 2. Projection of the unit cell of $La_{12}I_{17}Fe_2$ along [010] (infinite view) to illustrate the halide connectivity (La, gray circles; I, open circles).

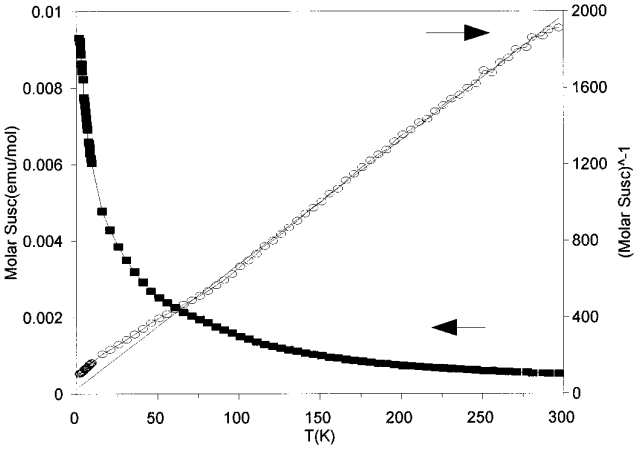

FIG. 3. Plots of $\chi - \chi_0$ (solid squares) and $1/(\chi - \chi_0)$ (empty circles) of $La_{12}I_{17}Fe_2$ as a function of temperature with the Curie–Weiss fit for $T > 100$ K.

bility, $\chi - \chi_0$, shown in Fig. 3 is fit well over about 75–300 K and gives, with $\mu = 2.83 \cdot \sqrt{C}$, a moment of 1.11(2) BM. The data at 1 T give 1.05 BM over 100–300 K. These are below the ideal spin-only value of 1.73 BM for one unpaired electron, but this difference could well result from spin-orbital coupling with such heavy cluster elements. This sort of behavior has been analyzed for a Mn-centered zirconium cluster chloride (18). The boundaries of the electron exchange frequency between 17- and 18-*e* clusters are not evident with present data, nor is any notion of whether this freezes out to produce an ordered superstructure at some lower temperature. Magnetic ordering is not evident >6 K. Any contribution of this cluster exchange to electronic conduction must be small judging from Q-measurements of resistivity at ~35 MH_z between 100 and 300 K, which data, though rather scattered, indicate a substantially temperature-independent value of ~350 $\mu\Omega \cdot$ cm. This is a lower limit too as the sample contained ca. 10% of the metallic LaI_2. ESR and structural measurements at low temperatures could be useful in the further pursuit of these electronic details.

The number of $R_{12}I_{17}Z_2$ compounds seems to be fairly limited, in contrast to the two structure types with discrete clusters, $R_7I_{12}Z$ and $R_6I_{10}Z$, that have been found for a wide range of rare-earth-metals, halides, and interstitial atoms. Despite many experimental efforts to expand the variety of these structurally and physically interesting examples, only four representatives have been synthesized. It seems that they form better under more reduced conditions in reactions that are rare-earth-metal richer than the stoichiometry requires. Competitive phases are $R_7I_{12}Z$ and the metallic RI_2 on the oxidized and reduced sides, respectively, while temperature and heating time apparently have little influence of the yields of the products, as the syntheses of $Pr_{12}I_{17}Fe_2$, $Pr_{12}I_{17}Re_2$, $La_{12}I_{17}Fe_2$, and $Ce_{12}I_{17}Mn_2$ under different reaction conditions demonstrate. The lack of many common interstitials in the series, especially of Mn with La and Pr, must arise from subtle differences in stabilities of these vs alternative products. The metal-rich compounds discussed here, with I : R ratios of 1.42 : 1, are the halogen-poorest among those phases that contain octahedral clusters interconnected only by halide bridges. These limits of course do not apply to clusters condensed via shared edges to form infinite chains (1–3) or in the bioctahedra in the recently discovered $A_2R_{10}I_{17}Z_2$ and $La_{10}I_{15}Os_2$ (19, 20). It should be noted that the known compound $Gd_{12}I_{17}C_6$, with the same I : R ratio as the phases described here, features a completely different structure, *cis*- and *trans*-edge-sharing Gd_6 clusters in the form of zigzag chains that are centered by a C_2 unit (21).

ACKNOWLEDGMENTS

The authors are indebted to J. Ostenson for measurement of the magnetic data and to D. C. Johnston for valuable discussions. This research was supported by the National Science Foundation, Solid State Chemistry, via Grants DMR-9207361 and DMR-9510278, and was carried out in the facilities of Ames laboratory, U.S. Department of Energy. M.L. is grateful to the Alexander von Humboldt Foundation for a Feodor Lynen Fellowship.

REFERENCES

1. J. D. Corbett, *in* "Modern Perspectives in Inorganic Crystal Chemistry" (E. Parthé, Ed.), p. 27. Kluwer Academic, Dordrecht, 1992.
2. J. D. Corbett, *J. Alloys Compd.* **224,** 10 (1995).
3. A. Simon, Hj. Mattausch, G. J. Miller, W. Bauhofer, and R. K. Kremer, *in* "Handbook on the Physics and Chemistry of Rare Earths" (K. A. Gschneidner Jr. and L. Eyring, Eds.), Vol. 15, p. 191. Elsevier, Amsterdam/New York, 1991.
4. M. W. Payne and J. D. Corbett, *Inorg. Chem.* **29,** 2246 (1990).
5. T. Hughbanks and J. D. Corbett, *Inorg. Chem.* **28,** 631 (1989).
6. R. Llusar and J. D. Corbett, *Inorg. Chem.* **33,** 849 (1994).
7. T. Hughbanks and J. D. Corbett, *Inorg. Chem.* **27,** 2022 (1988).
8. D. S. Dudis, J. D. Corbett, and S. -J. Hwu, *Inorg. Chem.* **25,** 3434 (1986).
9. S.-J. Hwu and J. D. Corbett, *J. Solid State Chem.* **64,** 331 (1986).
10. Y. Park and J. D. Corbett, *Inorg. Chem.* **33,** 1705, 3848 (1994).
11. J. D. Corbett, *Inorg. Synth.* **22,** 15, 31 (1983).
12. G. Meyer, *Chem. Rev.* **88,** 93 (1988).
13. TEXSAN, Version 6.0, Molecular Structure Corp., The Woodlands, Texas, 1990.
14. N. Walker and D. Stuart, *Acta Crystallogr.* **A39,** 159 (1983).
15. A. M. Guloy and J. D. Corbett, *Inorg. Chem.* **35,** (1996) in press.
16. M. Lulei and J. D. Corbett, *Inorg. Chem.* **35,** 4084 (1996).
17. M. Lulei and J. D. Corbett, *Z. Anorg. Allg. Chem.,* in press.
18. T. Hughbanks, G. Rosenthal, and J. D. Corbett, *J. Am. Chem. Soc.* **110,** 1511 (1988).
19. M. Lulei, P. A. Maggard, and J. D. Corbett, *Angew. Chem.,* in press.
20. M. Lulei, J. D. Martin, L. M. Hoistad, and J. D. Corbett, in preparation.
21. A. Simon and E. Warkentin, *Z. Anorg. Allg. Chem.* **497,** 79 (1983).